International journal of Engineering Research-Online
A Peer Reviewed International Journal
Articles available online http://www.ijoer.in

Vol.2., Issue.5, 2014

REVIEW ARTICLE

ISSN: 2321-7758

POWER QUALITY IMPROVING BY ENHANCING THE DYNAMIC PERFORMANCE OF DFIG USING SMES WITH ANN CONTROL TECHNIQUE

AKULA SREENU BABU[1*], SYED KARIMULLA[2], K.NARENDRA[3]
[1]PG Student,Departmentof EEE, Al Habeeb college of Engineering & Technology, Chevella, India.
[2]Asst Professor,Departmentof EEE, Al Habeeb college of Engineering & Technology, Chevella, India.
[3]Asst Professor, Department of EEE, P S C M R College of Engg. Technology ,Vijayawada, India.

Article Received: 16/09/2014
Article Revised on: 30/09/2014
Article Accepted on:01/10/2014

AKULA.SREENU BABU

SYED.KARIMULLA

K.NARENDRA

ABSTRACT

The integration of wind turbines into modern power grids has significantly increased during the last decade. Wind turbines equipped with doubly fed induction generators (DFIGs) have been dominating wind power installation worldwide since 2002. [1] In this paper, the dynamic performance of DFIG is improved during voltage sag and swell by using superconducting magnetic energy storage (SMES).SMES unit is a combination of converter and chopper. Hystresis current controller is used to control converter, fuzzy logic controller is used to control chopper. Detailed simulation is carried out by using MATLAB/SIMULINK software.

Key Words—Doubly fed induction generator (DFIG), fuzzy logic, hysteresis current controller (HCC), superconducting magnetic energy storage (SMES), voltage sag, voltage swell and wind energy conversion system (WECS).

INTRODUCTION

Utilization of renewable energy sources is becoming more attractive due to the detrimental impact of conventional energy resources on the environment. Implementation of carbon tax in some countries has also been considered as a trigger to accelerate the utilization of renewable energy sources [1]. One of the most promising renewable energy sources is wind energy, which has grown rapidly from about 2000 MW at the end of the year 1990 to 94000 MW by the end of the year 2007. The future prospects of the global wind industry are very encouraging, and it is estimated to grow by more than 70% to reach 160 GW by the year 2012. It is estimated that, by the year 2020, wind power will supply at least 10% of global electricity demands [2]. Owing to the rapid development of power electronics technology, the number of wind turbines equipped with converter stations has increased. The doubly fed induction generator (DFIG) is one of the most popular variable- speed wind turbine generators (WTGs). In this technology, the rotor winding is connected to a coupling transformer through a back-to-back partial-scale voltage source converter (VSC), whereas the stator winding is directly connected to the grid at a point of common coupling (PCC) through the coupling transformer. The VSC decouples the mechanical and electrical frequencies and make variable-speed operation possible [3].If generator is running super- synchronously, electrical power is delivered to the grid through both stator and the rotor. If generator is running sub-synchronously, electrical power is delivered into the rotor from grid. Global trend shows that the market share of the installed wind energy conversion system (WECS) has been dominated by DFIG-based wind turbines since 2002 [4]. In the earlier stages of integrating WECSs into the electricity grids, WTGs were disconnected from the grid during faults at the grid side to avoid any possible damages to wind turbines. Recently, existing WTGs, however, will have to be designed/managed to comply with the recent requirements of new grid codes [5] to assure the continuity of supplying power to the grid during transient and abnormal operating conditions. There are two strategies that can be applied to improve the performance or the fault ride through (FRT) capability of the DFIG. First is by developing new control techniques to fulfill the criterion of the transmission system operators, as presented in most of the literature [6]–[8]. However, this strategy is effective for new installation and new connection of WECSs to the grid. Second is by applying FACTS devices or storage energy systems, which are a more cost effective choice for existing WECSs. Variable- speed WECSs such as DFIG were introduced to overcome the weakness of the fixed-speed type in capturing maximum wind energy and to contribute in supplying reactive power to the grid when required. The advantages of variable speed wind turbine is that it reduces mechanical stresses adjust reactive power. Compared with full-scale variable- speed WECSs, DFIG is very sensitive to grid faults [7], where, even though the DFIGs are connected far away from the grid, the grid faults will influence the voltage profile at the PCC. Moreover, during grid fault, voltage drop at the DFIG terminal, high current flow at both grid and rotor side converters, and high voltage across the dc link capacitor may lead to converter station blocking. This condition will be ended by the disconnection of the DFIG from the system. If the DFIG contributes in delivering a large portion of power to the grid, financial loss will be uncountable. Most of the studies about the DFIG are concerned about the improvement of its FRT capability during voltage sag [6]–[9]. No attention however is given to improve the DFIG performance under voltage sag and voltage swell conditions using the same controller. Although the swell event in the grid side is rarely to occur, it can cause voltage rise at the PCC that may violate the grid codes' requirements. Recently, the maximum voltage ride through of Spain and Australia's grid codes is set to 1.3 pu. If the voltage profile at the PCC rises above 1.3 pu, the WTGs have to be disconnected from the grid. Since the successful installation of the 30-MJ superconduct- ing magnetic energy storage (SMES) unit at Bonneville power administration, Tacoma, in 1982 , SMES has attracted many researchers to study its potential applications in power systems . There are many papers in the literature that investigated the application of SMES to WECSs. However, most of these studies have only focused on the use of the SMES unit to smooth the output power of fixed-speed WECSs during wind speed fluctuation to avoid system instability . This paper presents a new application of the SMES unit to improve the performance of a wind turbine equipped with DFIG during voltage sag and voltage swell at the grid side. A new control system for the SMES unit based on hysteresis current control in conjunction with fuzzy logic control is proposed. The Simulink/Matlab software is used to simulate the wind turbine, the SMES unit, and the model under study. Results are analyzed to highlight the improved dynamic performance of WECSs in conjunction with the SMES unit.

II. SMES

An SMES system consists of a superconductor coil, a power-conditioning system, a cryogenic refrigerator, and a cryostat/vacuum vessel to keep the coil at a low temperature required to maintain it in superconducting state. T. Other advantages of the SMES [1] unit include very quick response and possibilities for high-power applications . A typical SMES configuration is shown in Fig. 1.

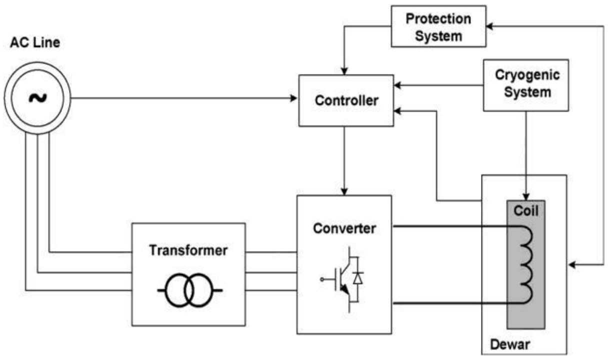

Fig. 1. Typical schematic diagram of an SMES unit.

III. SYSTEM UNDER STUDY

The system under study shown in Fig. 2(a) consists of six 1.5-MW DFIGs connected to the ac grid at the PCC. The DFIG consists of an induction generator with stator winding con- nected directly to the grid through a *Y* / step-up transformer, whereas the rotor winding is connected to a bidirectional back-to-back insulated gate bipolar transistor (IGBT) VSC, as shown in Fig. 2(b). The grid that is represented by an ideal three-phase voltage source of constant frequency is connected to the wind turbines via a 30-km transmission line and /*Y* step-up transformer. The reactive power produced by the wind turbines is regulated at zero MVar under normal operating conditions. For an average wind speed of 15 m/s, which is used in this study, the turbine output power is 1.0 pu, and the generator speed is 1.2 pu. The SMES unit is connected to the 25-kV bus and is assumed to be fully charged at its maximum capacity of 1.0 MJ Tables I and II.

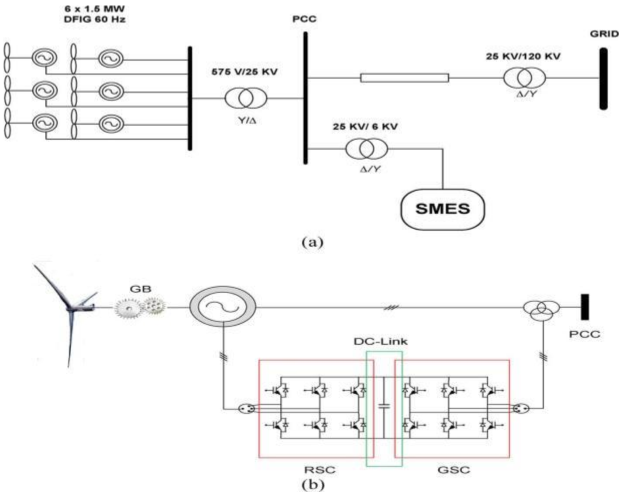

Fig. 2. (a) System under study. (b) Typical configuration of an individual DFIG

TABLE 1: PARAMETERS OF THE DFIG

Duty Cycle (D)	SMES Coil Action
D = 0.5	standby condition
$0 \leq D < 0.5$	discharging condition
$0.5 < D \leq 1$	charging condition

TABLE 2: parameters of the transmission line

Rated Power	9 MW (6 x @ 1.5 MW)
Stator Voltage	575 V
Frequency	60 Hz
R_S	0.023 pu
R_R	0.016 pu
V_{DC}	1150 V

IV. SMES CONTROL APPROACHES

Generally, there are two major configurations of SMES, i.e., current source converter (CSC) and VSC.

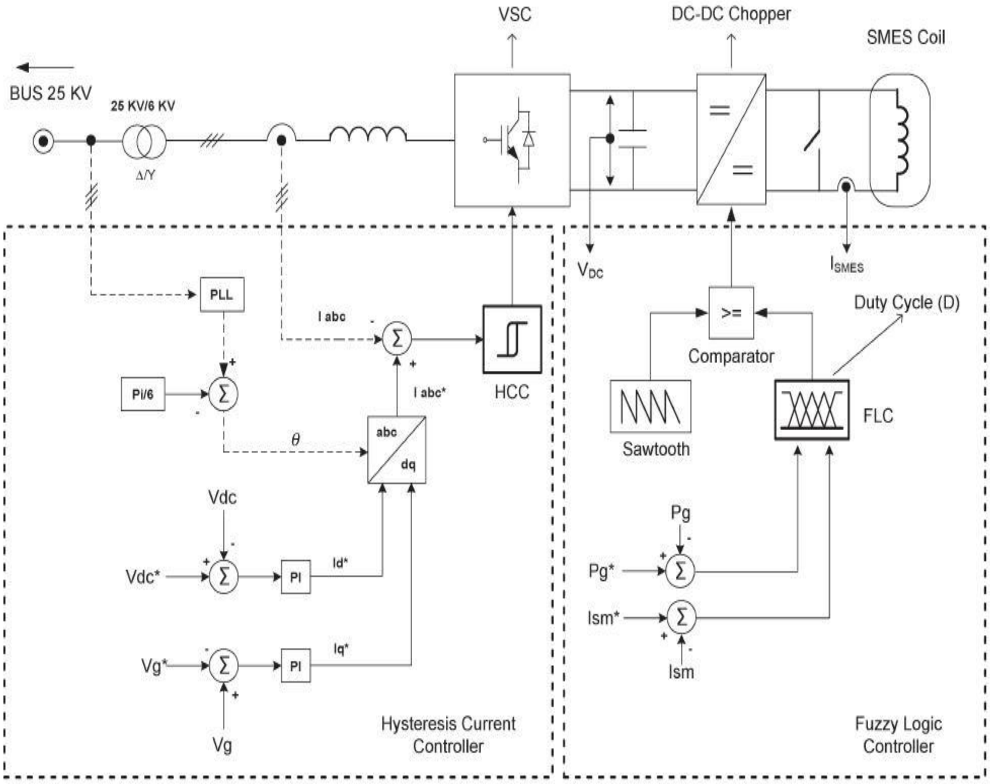

Fig. 3. SMES unit configuration and the proposed HCC–FLC control scheme.

Traditionally, CSC is connected through a 12-pulse converter configuration to elimi- nate the ac-side fifth and seventh harmonic currents and the dc- side sixth harmonic voltage, thus resulting in significant savings in harmonic filters . However, because this configuration uses two 6-pulse CSCs that are connected in parallel, its cost is relatively high. The VSC, on the other hand, must be connected with a dc–dc chopper through a dc link, which facilitates energy exchange between the SMES coil and the ac grid. Reference estimates the total cost of the switching devices of the CSC to be 173% of the switching devices and power diodes required for equivalent capacity of the VSC and the chopper. Moreover, a VSC has a better self-commutating capability, and it injects lower harmonic currents into the ac grid than a comparable CSC. The use of IGBTs in this configuration is more beneficial than GTO since the switching frequency of an IGBT lies on the range of 2–20 kHz, whereas, in case of GTO, the switching frequency cannot exceed 1 kHz [3][4][5].

The proposed SMES configuration used in this paper consists of a VSC and dc–dc chopper, as shown in Fig. 3. The converter and the chopper are controlled using a hysteresis current con- troller (HCC) and a fuzzy logic controller (FLC), respectively. The stored energy in the SMES coil can be calculated as

$$E = \frac{1}{2} I_{SMES}^2 L_{SMES} \qquad (1)$$

where E, ISMES , and LSMES are the stored energy, current, and coil inductance of the SMES unit, respectively. While the control system of the dc–dc chopper is presented in , the control approach for the VSC as part of the SMES configuration is not presented.The configuration of SMES in is new, but its application is limited for low WTG capacity, and since the SMES coil is proposed to be connected to the individual DFIG's converters, this topology will be only appropriate for new WECS installations. Application of the SMES system to microgrids is presented in , where the SMES is used to stabilize the entire microgrid system. The control scheme presented in this work is very complex because it is working for three different levels of controls; this will lead to high implementation and maintenance cost. Moreover, it requires a robust computational system.

The proposed control algorithm in this paper is much simpler and closer to realistic applications. In the aforementioned papers, four proportional-integral (PI) controllers are proposed, which require more computational time to optimally tune its parameters to maintain overall system stability and to achieve satisfactory dynamic response during transient events. More- over, the control system for the dc–dc chopper in these studies considered only the DFIG-generated active power (PG) as a control parameter, but it ignored the energy capacity of the SMES unit. The control scheme in this paper comprises only two PI controllers and considers the SMES coil current to take the SMES stored energy capacity into account, along with the DFIG generated power as control parameters to determine the direction and level of power exchange between the SMES coil and the ac system. This control system is efficient, simple, and easy to implement, as will be elaborated here.

A. HCC

The HCC is widely used because of its simplicity, insen-sitivity to load parameter variations, fast dynamic response, and inherent maximum-current-limiting characteristic . The basic implementation of the HCC is based on deriving the switching signals from the comparison of the actual phase current with a fixed tolerance band around the reference current associated with that phase. However, this type of band control is not only depending on the corresponding phase voltage but is also affected by the voltage of the other two phases. The effect of interference between phases (referred to as interphase dependence) can lead to high switching frequencies. To maintain the advantages of the hysteresis methods, this phase dependence can be minimized by using the phase-locked loop (PLL) technique to maintain the converter switching at a fixed predetermined frequency level . [1][2] The proposed SMES with an auxiliary PLL controller is shown in Fig. 3. The HCC is comparing the three-phase line currents (Iabc) with the reference currents (I* abc), which is dictated by the I* d and I*q references. The values of I*d and I*q are generated through conventional PI controllers based on the error values of Vdc and Vs. The value of I* d and I* q is converted through Park transformation (dq0 − abc) to produce the reference current (I* abc).

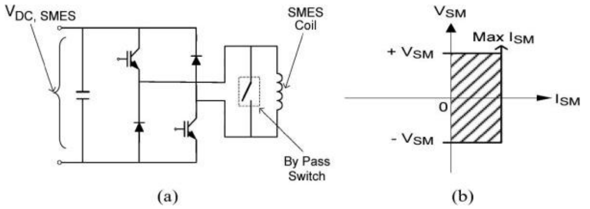

Fig. 4. (a) Class-D dc–dc chopper topology with an SMES coil. (b) Operation range of the SMES coil

B. FLC

To control power transfer between the SMES coil and the ac system, a dc–dc chopper is used, and fuzzy logic is selected to control its duty cycle (D), as shown in Fig. 3. The FLC is developed according to the fuzzy inference flowchart shown in Fig. 4, which is a process of formulating the mapping from a given input to the designated output. Input variables for the model are the real power generated by the DFIG and the SMES coil current. The output of the FLC is the duty cycle (*D*) for a class-D dc–dc chopper that is shown in Fig. 5(a). The *V – I* operational range for the SMES coil is shown in Fig 5(b). The duty cycle determines the direction and the magnitude of the power exchange between the SMES coil and the ac system, as presented in Table III. If the duty cycle (*D*) is equal to 0.5, no action will be taken by the coil, and the system is under normal operating conditions. Under this condition, a bypass switch that is installed across the SMES coil [shown in Fig. 4(a)] will be closed to avoid the draining process of SMES energy during normal operating conditions. The bypass switch is controlled in such a way that it will be closed if *D* is equal to 0.5; otherwise, it will be opened. This technique has been introduced in some studies in the literature . When the grid power is reduced, *D* will be reduced accordingly to be in the range of 0–0.5, and the stored energy in the SMES coil will be transferred to the ac system. The charging process of the SMES coil takes place when *D* is in the range of 0.5–1.

TABLE3: RULES OF THE DUTY CYCLE

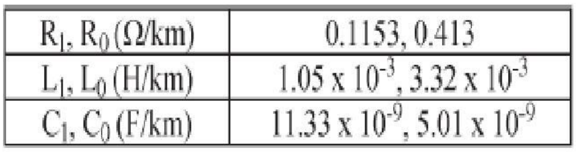

R_1, R_0 (Ω/km)	0.1153, 0.413
L_1, L_0 (H/km)	1.05×10^{-3}, 3.32×10^{-3}
C_1, C_0 (F/km)	11.33×10^{-9}, 5.01×10^{-9}

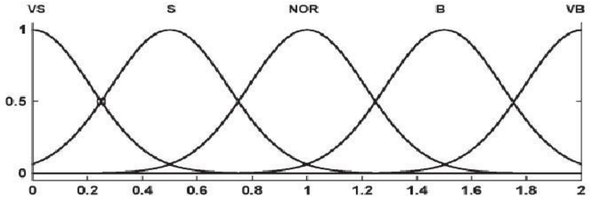

Fig.5 MF for the input variable P_G(pu)

The relation between *V*SMES and *V*DC,SMES can be written as

$$V_{SMES} = (1 - 2D)V_{DC,SMES} \quad (2)$$

where *V*SMES is the average voltage across the SMES coil, *D* is duty cycle, and *V*DC,SMES is the average voltage across the dc-link capacitor of the SMES configuration

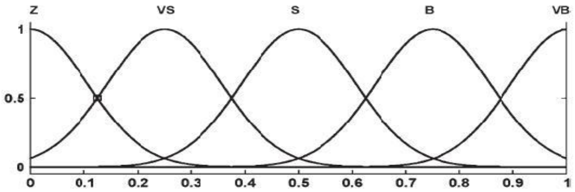

Fig.6. MF for the input variable I_{SMES}(pu)

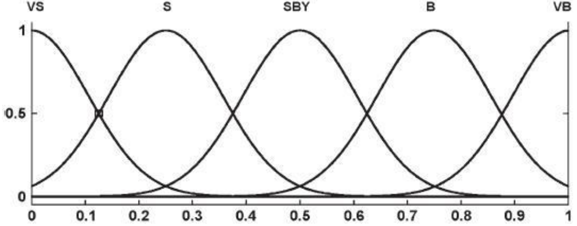

Fig.7.MF for the output variable D(duty cycle).

V. SIMULATION RESULTS AND DISCUSSION

A. Voltage Sag Event

A voltage sag depth of 0.5 pu lasting for 0.05 s is applied at *t* = 2 s at the grid side of the system under study [Fig. 2(a)]. Without the SMES unit, the real power produced by the DFIG will drop to 0.6 pu, and it reaches a maximum overshooting of 40% during the clearance of the fault, as shown in Fig 8(a). As can be seen in Fig 9(d), with the SMES unit connected to the system, the DFIG output power will drop to only 0.875 pu. Fig. 9(f) implies that,with the connection of the SMES unit and during the event of voltage sag, the reactive power support by the DFIG is reduced, and the steady-state condition is reached faster, compared to the system without SMES. The voltage at the PCC is shown in Fig. 8(c), where without SMES, voltage will drop to 0.6 pu. However, by connecting the SMES unit, voltage drop at the PCC will be reduced to only 0.8 pu as shown in Fig 9(g), which will lead to a voltage drop at the generator terminal to a level of 0.8 pu, Fig. 9(e). The voltage overshoot across the dc-link capacitor during fault clearance is slightly reduced with the SMES unit connected to the system..

B. Voltage SWELL Event

Voltage swell can occur due to switching off a large load or switching on a large capacitor bank. [1][2] In this simulation, a voltage swell is applied by increasing the voltage level at the grid side to 1.5 pu. The voltage swell is assumed to start at *t* = 2 s and lasts for 0.05 s. In this event, the DFIG-generated power will increase upon the swell occurrence and will be reduced when it is cleared, as shown in Fig. 11(e).The maximum power overshoot is slightly reduced with the SMES unit connected to the system. To compensate for the voltage rise, DFIG will absorb the surplus reactive power, as shown in Fig. 11(f). The amount of reactive power absorbed by the DFIG is lesser with SMES connected to the PCC since the voltage profile at the PCC is rectified to a level below 1.3 pu with the connection of the SMES unit, whereas this voltage will remain above 1.3 pu without SMES connected to the PCC [Fig. 10(c)]. Without the connection of the SMES unit, the voltage at the PCC does not comply with the high voltage ride through (HVRT) of Spain and Australia grid codes], which will lead to the disconnection of the DFIG from the system.

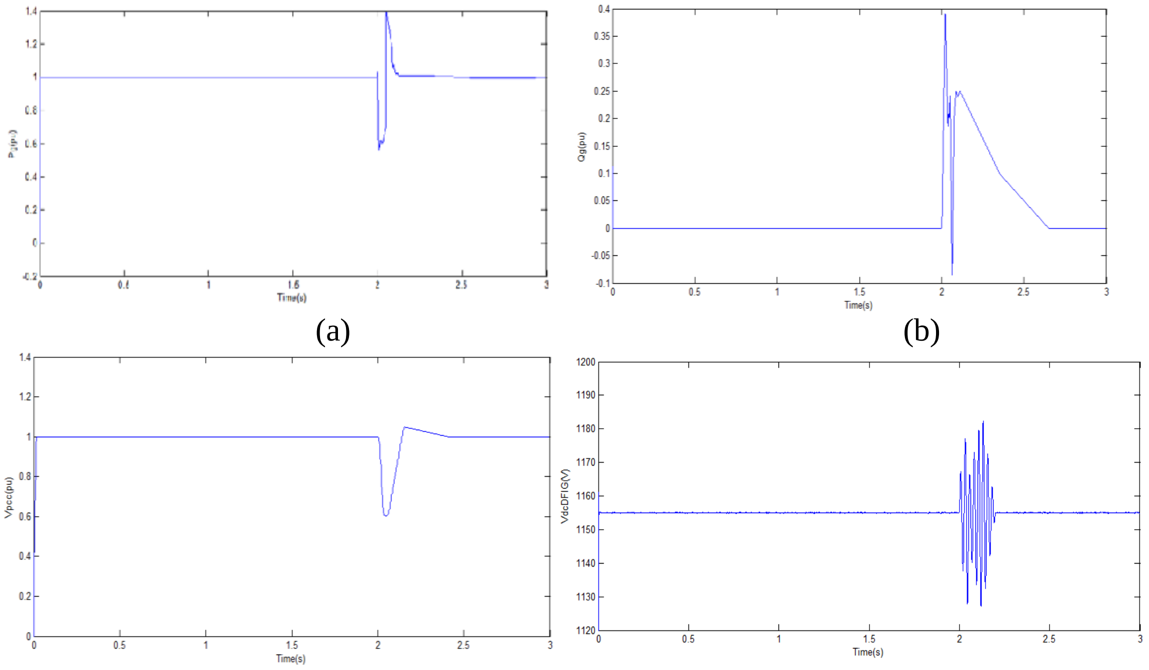

(a) (b)

(c) (d)

Fig. 8. DFIG responses during voltage sag without an SMES unit.(a) Active power. (b) Reactive power. (c) PCC voltage. (d) voltage at dc-link of dfig.

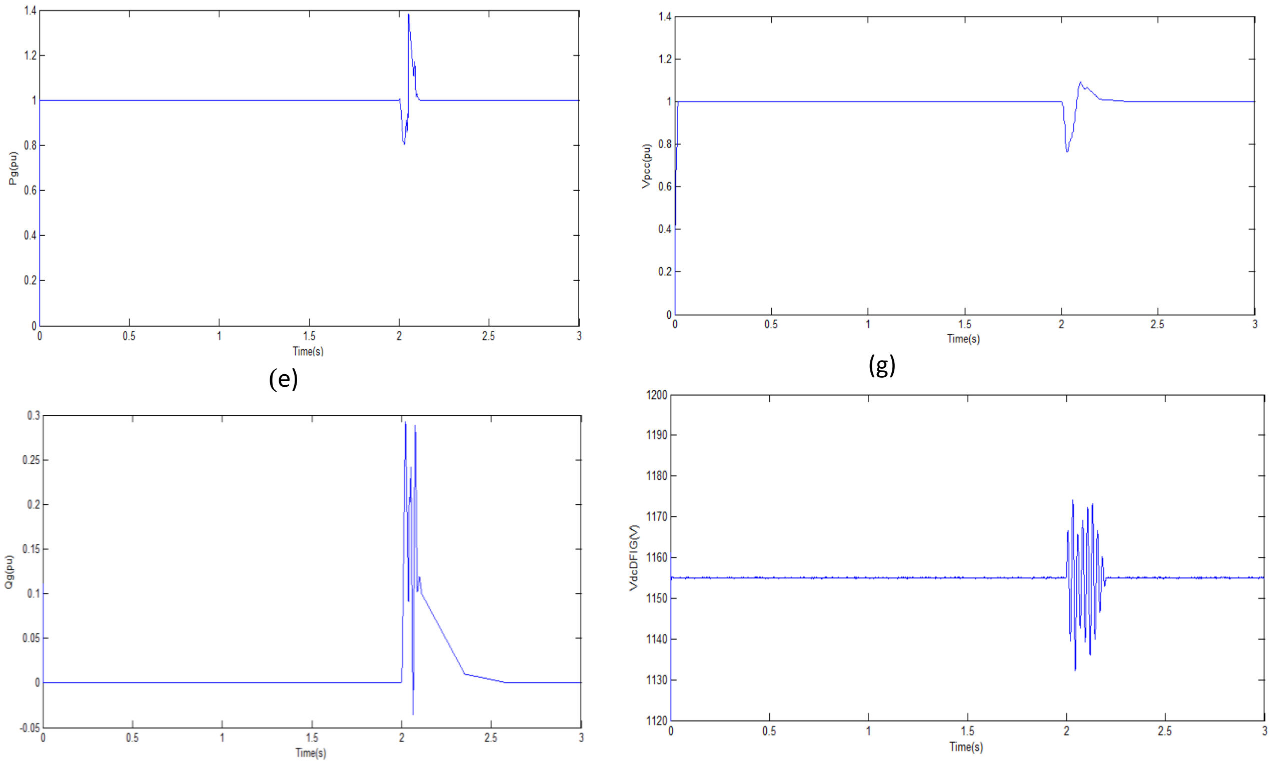

(e) (g)

(f) (h)

Fig. 9. DFIG responses during voltage sag with an SMES unit.(a) Active power. (b) Reactive power. (c) PCC voltage.(d) voltage at dc-link of dfig.

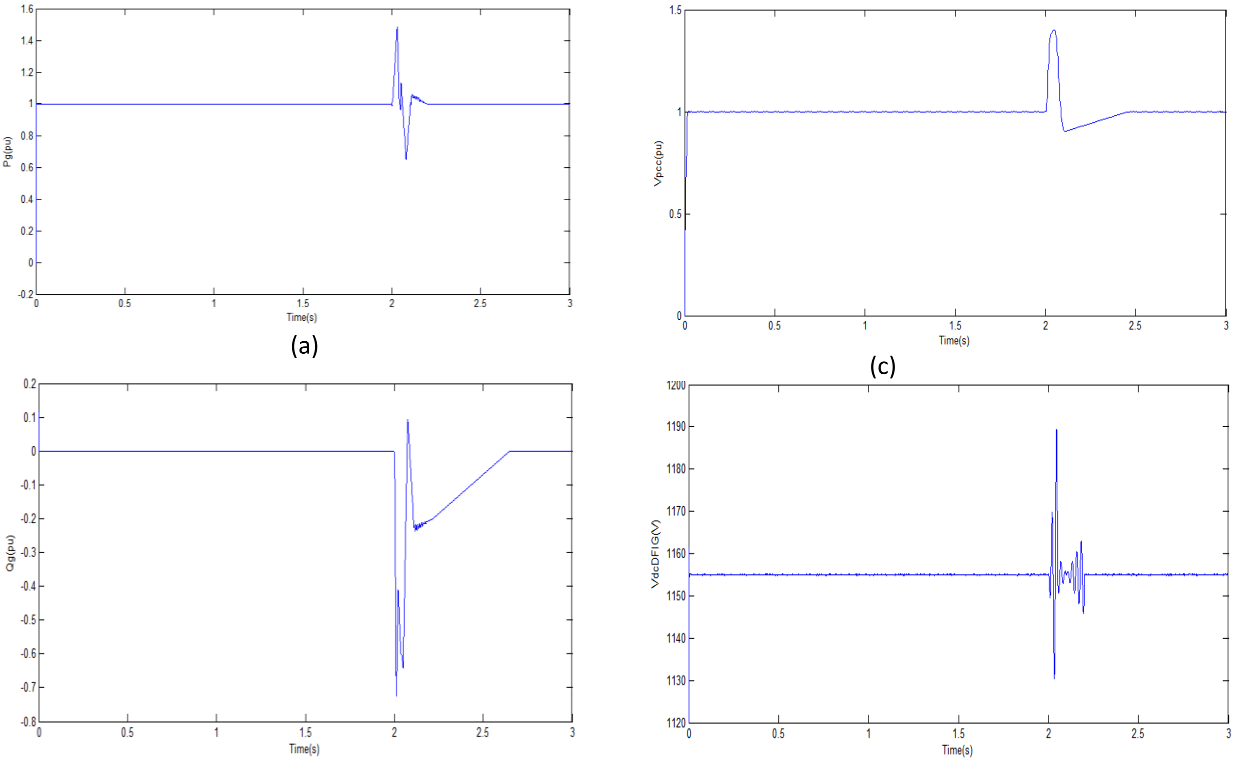

(a) (c)

(b) (d)

Fig. 10. DFIG responses during voltage swell without an SMES unit.(a) Active power. (b) Reactive power. (c) PCC voltage. (d) voltage at dc-link of dfig.

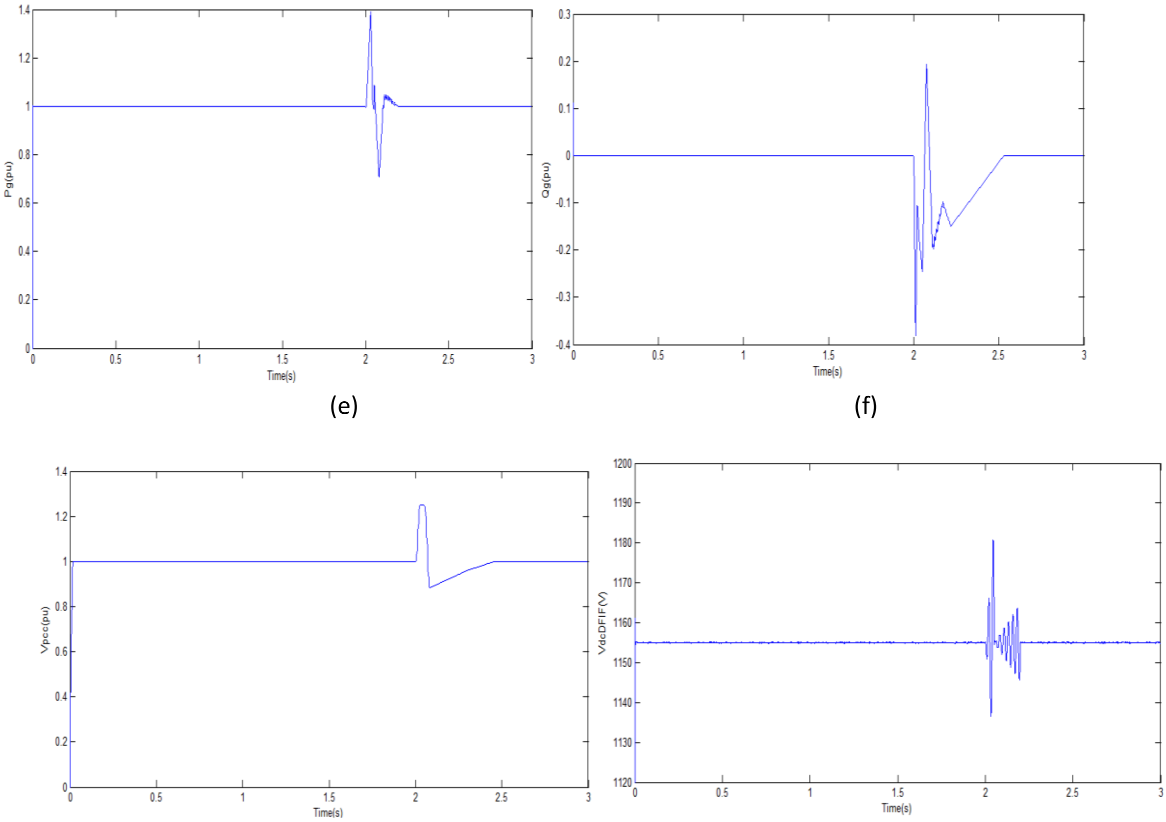

(e) (f)

(g) (h)

Fig. 11. DFIG responses during voltage swell with an SMES unit.(a) Active power. (b) Reactive power. (c) PCC voltage.

The extension of this project for voltage sag can be done with is the help of artificial neural network(ANN) which will show the better performance compared with fuzzy logic controller(FLC).The simulation waveforms of active power,reactive power,PCC voltage and vltage at dc-link of dfig as shown below

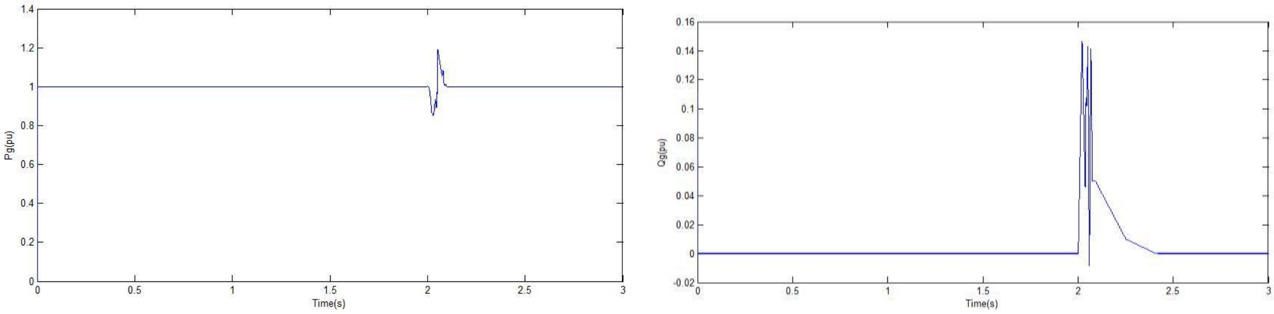

(a) (b)

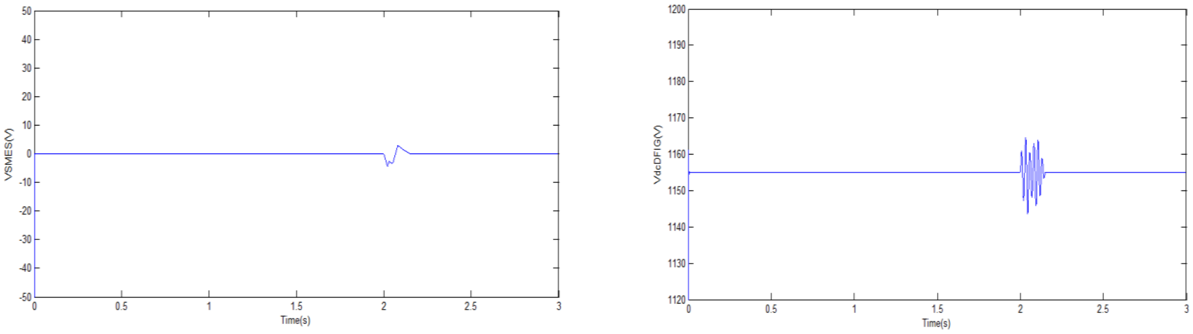

(b) (d)

Fig.12.(a)active power,(b)reactive power,(c)PCC voltage,(d)voltage at dc-link of dfig. c)PCC voltage (d) voltage at dc-link of dfig.

CONCLUSION

A new control algorithm along with a new application of the SMES unit to improve the transient response of WTGs equipped with DIFG during voltage sag and voltage swell events has been proposed. Simulation results have shown that the [1][2] SMES unit is very effective in improving the dynamic performance of a power system with wind turbine equipped with DFIG during voltage sag and voltage swell at the grid side. The proposed control algorithm of the SMES unit is simple and easy to implement and is able to improve the FRT of the DFIG. The extension of this project for voltage sag is done with the help of artificaial neural network(ANN).

REFERENCES

[1]. K.MasthanRao,P.D.V.S.K.Kishore " Improving Power Quality to Enhance the Dynamic Performance of DFIG by Using SMES" International Journal of Technology and Engineering Science, Vol 1 (5), pp 415 – 421, August 2013

[2]. A. M. Shiddiq Yunus, Mohammad A. S. Masoum,and A. Abu-Siada "Application of SMES to Enhance the DynamicPerformance of DFIG DuringVoltage Sag and Swell" IEEE TRANSACTIONS ON APPLIED SUPERCONDUCTIVITY, VOL. 22, NO. 4, AUGUST 2012

[3]. P. Musgrove, Wind Power. New York: Cambridge Univ. Press, 2010, pp. 221–222.

[4]. J. M. Carrasco, L. G. Franquelo, J. T. Bialasiewicz,

[5]. E. Galvan, R. C. P. Guisado, M. A. M. Prats, J. I. Leon, and N. Moreno-Alfonso, "Power-electronic systems for the grid integration of renewable energy sources: A survey," IEEE Trans. Ind. Electron., vol. 53, no. 4, pp. 1002–1016,jun.2006.

[6]. T. Ackerman, Wind Power in Power System. West Sussex,U.KWiley, 2005, p. 65.

[7]. M. Tsili and S. Papathanassiou, "A review of grid code technical requirements for wind farms," IET Renew. Power Gener., vol. 3, no. 3, pp. 308–332, Sep. 2009.

[8]. S. Seman, J. Niiranen, and A. Arkkio, "Ride-through analysis of dou- bly fed induction wind-power generatorunder unsymmetrical network disturbance," IEEE Trans. Power Syst., vol. 21, no. 4, pp. 1782–1789, Nov. 2006.

[9]. J. Lopez, E. Gubia, E. Olea, J. Ruiz, and L. Marroyo, "Ride through of wind turbines with doubly fed induction generator under symmetrical voltage dips," IEEE Trans. Ind. Electron., vol. 56, no. 10, pp. 4246–4254, Oct. 2009.

[10]. M. Mohseni, S. M. Islam, and M. A. S. Masoum, "Impacts of sym- metrical and asymmetrical voltage sags on DFIG-based wind tur- bines consideringphase-angle jump, voltage recovery, and sag para- meters," IEEE Trans. Power Electron., vol. 26, no. 5, pp. 1587–1598, May 2011.